Multirate and Model Predictive Control of a Pneumatic Isolation Table with a Discrete Actuator

Yuichi Chida * **Nijihiko Ishihara** * **Masaya Tanemura** *

* *Shinshu University, Nagano, 3808553 Japan (e-mail: chida@shinshu-u.ac.jp).*

Abstract: This study addresses the control problem for a pneumatic isolation table system that includes a discrete valued input actuator. Control performance occasionally deteriorates if it is impossible to use an adequate high sampling frequency for the system. A combined method of multirate control and model predictive control is proposed to improve control performance if the sampling frequency to measure outputs is insufficiently low. The effectiveness of the proposed method is verified via numerical simulations for a pneumatic isolation table system model.

Keywords: Pneumatic systems, Discontinuous control, Multirate, Model predictive control, Quantized signals.

1. INTRODUCTION

Pneumatic isolation tables are used in numerous manufacturing fields, and active controls are used to apply appropriate damping effects to the tables by changing the internal pressure of the air springs(Kato et al., (2010, 2007)). Several studies have investigated control for a pneumatic isolation table (Koike et al., (2013); Maruyama et al., (2015); Kato et al., (2007); Jong and Kwang, (2013); Marcel et al., (2006); Kawashima et al., (2007)). In order to change the pressure of the springs, servo valves or on/off valves are used as actuators to control the inflow or outflow of the springs. On/off valves are extremely low in cost relative to servo valves although it is difficult to obtain sufficient active control performance by the on/off valves because the controlled plant is driven by discrete input values. The study addresses the control problem for a plant that includes a discrete input actuator. For the control problem, several control methods are proposed and include a dynamical optimal quantizer(Minami et al., (2007); Azuma and Sugie, (2007, 2008); Sawada and Shin, (2010)) or feedback modulation method(Ishikawa et al., (2007)), or a Lyapunov-function based method(Koike et al., (2013); Koike and Chida, (2012); Maruyama et al., (2013, 2015)). Furthermore, a few nonlinear model predictive control approaches are executed for process control systems(James and Michael, (2017); Kobayashi et al., (2014)).

Conversely, in the present study, we initially indicate that the control performance deteriorates if it is impossible to use sufficiently high sampling frequency for a pneumatic isolation table control system with on/off valves. The reason as to why the performance deteriorates is attributed to the insufficient resolution of control input because the input is simultaneously quantitatively and temporally discretized. In the case in which the resolution of the quantized value and sampling period are both coarse, it is not possible to inject the control input while maintaining

sufficient system precision. Therefore, it is inadequate to use a low sampling frequency for the discrete valued input system. However, sampling frequency is sometimes low in cases when processors with relatively poor calculation performance are used or when control methods with large calculation costs such as model predictive control (MPC) are adopted. In order to improve control performance, multirate control(Fujimoto, (2009); Martin et al., (1988)) is adopted that includes high sampling frequency for control input updating in the face of low sampling to measure outputs. In this case, the determination of the multirate control input is another control problem in the aforementioned cases. In order to solve the control problem, MPC-based method(Maruyama et al., (2013, 2015)) is adopted. Hence, we propose a control method of multirate control based MPC method to improve control performance for a low sampling frequency system to measure outputs. The effectiveness of the proposed method is verified via numerical simulations for a model of a pneumatic isolation table control system. The proposed method is appropriate for a control system that cannot use a high sampling frequency to measure outputs although high sampling can be used for the control input.

2. PLANT

In the study, the following single input discretized plant $\tilde{G}$ is considered.

$$\tilde{G} : \tilde{\boldsymbol{x}}[k+1] = \tilde{\boldsymbol{A}}\tilde{\boldsymbol{x}}[k] + \tilde{\boldsymbol{B}}u[k] \tag{1}$$

$\tilde{G}$ denotes a linearized model of a nonlinear plant, such as a pneumatic isolation table, as shown in Section 5. Where, $k \in \{0\} \cup \mathbb{N}_+$, $\tilde{\boldsymbol{x}} \in \mathbb{R}^{N \times 1}$, and $u \in \mathbb{R}$ denote the step number of the discrete system, state variable, and control input, respectively. It is assumed that $(\tilde{\boldsymbol{A}}, \tilde{\boldsymbol{B}})$ is controllable and $\tilde{\boldsymbol{x}}$ is measurable and that the control input is added to the plant via a quantizer $\phi : \mathbb{R} \to \mathbb{R}$ that transforms the continuous input signal $\sigma[k]$ to the discretized one $u[k] = \phi(\sigma[k])$ as follows:
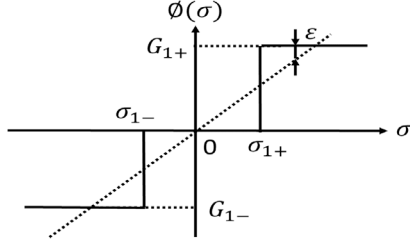
Fig. 1. Quantizer

$$u[k] = \phi(\sigma[k]), \qquad (2)$$

where ϕ satisfies $\phi(0) = 0$. An example of a quantizer is shown in Fig. 1, and it is assumed that the input consists of three discretized values, namely G_{1+}, 0, and G_{1-}.

3. OUTLINE OF THE STUDY

When we used the quantized input shown in Fig. 1, the control performance depended on the sampling frequency of the discretized plant. If the sampling frequency remains low, then good control performance cannot be achieved for the discretized control input system. However, one issue is that a relatively low sampling frequency is occasionally required in some cases. An example of this type of control situation is the case in which we use a control law with high calculation cost such as MPC. Another situation is when it is necessary to use low-performance control devices instead of high calculation performance control devices such as DSP. In this study, a control problem is considered in which the sampling frequency for output measurement remains low because of the above mentioned conditions. We propose a control method to overcome the restricted sampling frequency for the discretized input plant. The proposed control method consists of multirate control and MPC.

4. PROPOSED CONTROL METHOD

4.1 Multirate control

A block diagram of the multirate control system is shown in Fig. 2. The sampling period for the measurement of $\tilde{\boldsymbol{x}}[k]$ corresponds to T_y, and the interval of the zero-order-hold for control input corresponds to T_u. In this study, it is assumed that $T_y > T_u$, $n = T_y/T_u$, and n corresponds to a positive integer. Relationship between input and output is shown in Fig. 3. In Fig. 3, k denotes the step number for the control input, and the control input $\boldsymbol{U}[k]$ is defined as follows:

$$\boldsymbol{U}[k] := [u[k], u[k+1], \cdots, u[k+n-1]]^T. \qquad (3)$$

The problem corresponds to the determination of the control input $\boldsymbol{U}[k]$. Thus, we use the MPC method.

4.2 Multirate control law based on MPC

In this section, we describe the proposed control input decision method. It should be noted that the input of the plant corresponds to discretized values as shown in Fig. 1. The MPC method for a discretized input system was proposed by Maruyama et al., (2013, 2015). The
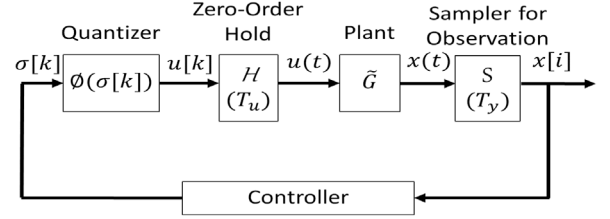

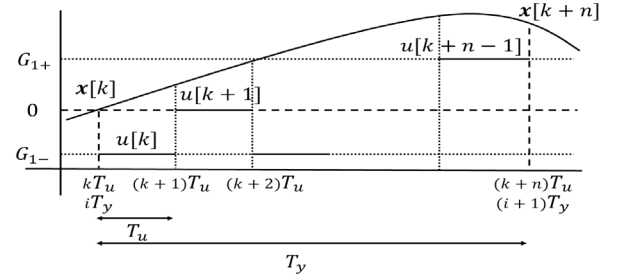Fig. 2. Block diagram of the multirate control system

Fig. 3. Sampling period of the multirate input and output

method is not suitable for the multirate input system, but we applied this method with a little modification in our study. The outline of the method is as follows. A positive quadratic cost function is introduced as follows:

$$V[k] = \tilde{\boldsymbol{x}}^T[k]\boldsymbol{P}\tilde{\boldsymbol{x}}[k], \qquad (4)$$

where $\boldsymbol{P} > 0$ denotes a solution of the discretized Lyapunov equation as follows:

$$(\tilde{\boldsymbol{A}} - \tilde{\boldsymbol{B}}\boldsymbol{F})^T\boldsymbol{P}(\tilde{\boldsymbol{A}} - \tilde{\boldsymbol{B}}\boldsymbol{F}) - \boldsymbol{P} = -\boldsymbol{Q}_L. \qquad (5)$$

Additionally, $\boldsymbol{F}$ denotes a feedback gain such that $\tilde{\boldsymbol{A}} - \tilde{\boldsymbol{B}}\boldsymbol{F}$ becomes Hurwitz, and $\boldsymbol{Q}_L$ denotes a specified arbitrary positive definite matrix. We focus on the cost function that corresponds to n step after,

$$V[k+n] = \tilde{\boldsymbol{x}}^T[k+n]\boldsymbol{P}\tilde{\boldsymbol{x}}[k+n]. \qquad (6)$$

We use (1), and $\tilde{\boldsymbol{x}}[k+n]$ is represented as follows:

$$\tilde{\boldsymbol{x}}[k+n] = \tilde{\boldsymbol{A}}^n\tilde{\boldsymbol{x}}[k] + \tilde{\boldsymbol{A}}^{n-1}\tilde{\boldsymbol{B}}u[k] + \tilde{\boldsymbol{A}}^{n-2}\tilde{\boldsymbol{B}}u[k+1]$$
$$+ \cdots + \tilde{\boldsymbol{B}}u[k+n-1] \qquad (7)$$
$$= \boldsymbol{A}_m\tilde{\boldsymbol{x}}[k] + \boldsymbol{B}_m\boldsymbol{U}[k] \qquad (8)$$
$$\boldsymbol{A}_m := \tilde{\boldsymbol{A}}^n \;,\; \boldsymbol{B}_m := [\tilde{\boldsymbol{A}}^{n-1}\tilde{\boldsymbol{B}}, \tilde{\boldsymbol{A}}^{n-2}\tilde{\boldsymbol{B}}, \cdots, \tilde{\boldsymbol{B}}].$$

We substitute (8) to (6) and we obtain the following expression:

$$\begin{aligned}
V[k+n] &= \tilde{\boldsymbol{x}}^T[k+n]\boldsymbol{P}\tilde{\boldsymbol{x}}[k+n] \\
&= (\boldsymbol{A}_m\tilde{\boldsymbol{x}}[k] + \boldsymbol{B}_m\boldsymbol{U}[k])^T\boldsymbol{P}(\boldsymbol{A}_m\tilde{\boldsymbol{x}}[k] + \boldsymbol{B}_m\boldsymbol{U}[k]) \\
&= \tilde{\boldsymbol{x}}^T[k]\,\boldsymbol{A}_m^T\,\boldsymbol{P}\boldsymbol{A}_m\tilde{\boldsymbol{x}}[k] + 2\tilde{\boldsymbol{x}}^T[k]\boldsymbol{A}_m^T\boldsymbol{P}\boldsymbol{B}_m\boldsymbol{U}[k] \\
&\quad + \boldsymbol{U}^T[k]\boldsymbol{B}_m^T\boldsymbol{P}\boldsymbol{B}_m\boldsymbol{U}[k], \qquad (9)
\end{aligned}$$

where the first term of (9) is independent of the control input, and thus we focus on the second and third terms. The following cost function is reintroduced as a renewed cost function as follows:

$$J(\boldsymbol{U}[k]) = 2\tilde{\boldsymbol{x}}^T[k]\boldsymbol{Y}\boldsymbol{U}[k] + \boldsymbol{U}^T[k]\boldsymbol{X}\boldsymbol{U}[k] \qquad (10)$$
$$\boldsymbol{X} := \boldsymbol{B}_m^T\boldsymbol{P}\boldsymbol{B}_m, \boldsymbol{Y} := \boldsymbol{A}_m^T\boldsymbol{P}\boldsymbol{B}_m.$$
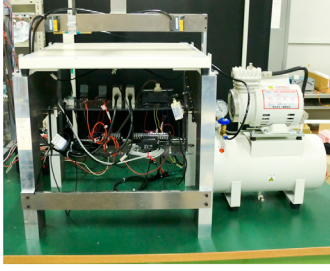
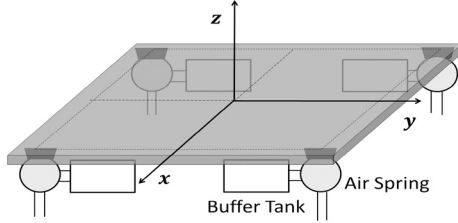Fig. 4. Experimental system of the pneumatic isolation table
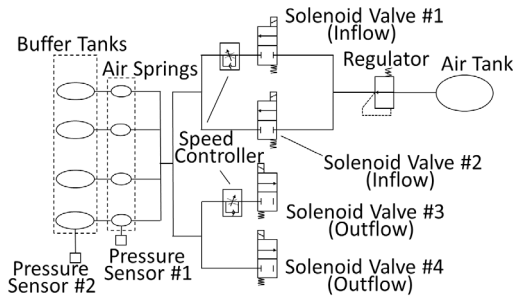

Fig. 5. Table model

Fig. 6. Pneumatic circuit

Subsequently, we obtain the optimal solution for minimizing $J(\boldsymbol{U}[k])$ by selecting $\boldsymbol{U}[k]$ via the real-time optimization method. It is difficult to obtain the optimal $\boldsymbol{U}[k]$ because the input value is discretized, and thus we determine the closest possible suboptimal solution via real-time searching calculations. The real-time searching calculation algorithm is given in Maruyama et al., (2013, 2015), and the calculation algorithm is applied for the study. In this case, n is specified such that $n \leq N$ to ensure the convexity of J, where N is the order of the state variable. If $\boldsymbol{U}[k] = 0$, then $J(\boldsymbol{U}[k]) = 0$. Otherwise, $J(\boldsymbol{U}[k]) < 0$ because $\boldsymbol{U}[k]$ is selected such that $J(\boldsymbol{U}[k])$ corresponds to the minimum. It is possible to modify the control law such that $\boldsymbol{U}[k]$ is applied for the plant if an additional condition that $V[k+n] - V[k] < 0$ is satisfied.

5. APPLICATION IN PNEUMATIC ISOLATION TABLE CONTROL

5.1 Configuration of the pneumatic isolation table system

The plant is a pneumatic isolation table system as shown in Fig. 4. The table is supported by four air springs. An sketch of the air springs is shown in Fig. 5. Each spring is connected to a buffer tank. The vertical translational motion and two rotational motions of the table are controlled by changing the inner pressure of the air springs
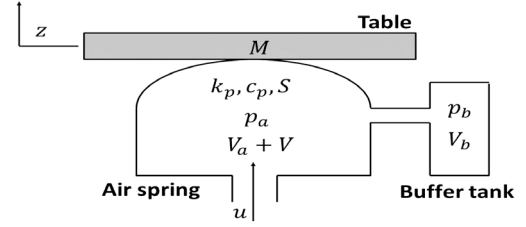

Fig. 7. Air spring model

using solenoid valves. In the study, we focus on the vertical translational motion, and rotational motion is ignored. The air circuit of the pneumatic isolation table system is represented in Fig. 6. The internal pressure of the springs is controlled by changing mass flow rate via the air pipes by using the valves. Air simultaneously flows into the four springs from the air tank by opening the solenoid valve #1 and #2. The valves operate in two modes such as opening or closing the valves. Conversely, air in the springs is exhausted by using valves #3 and #4 that are open at the same time.

Vertical displacement of table, z, is measured via a displacement sensor. Velocity, $\dot{z}$, is obtained by on-line derivation calculation. The internal pressure of the spring, p_a, and that of the buffer tank, p_b, are measured by pressure sensors. In the study, it is assumed that the inner pressure of the four air springs correspond to identical values, p_a, and that of the buffer tanks also correspond to common value, p_b. The system includes an approximate time delay of 10 ms due to the response of the valves and air pipe length.

The control input is calculated by using a DSP system, and the sensor signals are input to the DSP system via a 16-bit ADC. Additionally, control input is provided to the valves through DIO.

5.2 Model of plant

Models of the table and spring are shown in Fig. 5 and Fig. 7. The table is supported by four springs. However, it is assumed that an equivalent spring is used in the model indicated as Fig. 7 because we only focus on the vertical translation motion in the present study. Equation of motion based on the thermodynamic equilibrium conditions is described as follows:

$$M\ddot{z} + c_p\dot{z} + k_p z = Sp_a \qquad (11)$$

$$\dot{p}_a = \frac{\kappa R_s T_s}{(z_a + h_p z)S}(u(t - L) - \mu(p_a - p_b))$$
$$\quad - \frac{\kappa(p_0 + p_a)}{z_a + h_p z}h_p\dot{z} \qquad (12)$$

$$\dot{p}_b = \frac{\kappa R_s T_s}{z_b S}\mu(p_a - p_b), \qquad (13)$$

where z and u denote the vertical displacement of the table and mass flow rate of the flowing air, respectively, and correspond to the control input. Additionally, p_a and p_b denote the deviation of the internal pressure of the spring and buffer tank from the equilibrium p_0, respectively. All the variables are measurable, and $\dot{z}$ is obtained by the deviation using z. Specifically, M, k_p, c_p, S, R_s, κ, T_s,

μ, L, z_a, and z_b correspond to the parameters shown in Table 1. Here, $L = 20$ ms denotes the time delay that includes input delay via air transmission, 10 ms, and the calculation time delay for the control input calculation. We assume that $z_a \gg h_p z$ and $p_0 \gg p_a$ are satisfied in the present study, and (12) is approximated as follows:

$$\dot{p}_a = K_{gp}u(t - L) - K_{zp}\dot{z} - K_a p_a + K_a p_b, \quad (14)$$

where $K_{gp} = \frac{\kappa R_s T_s}{z_a S}$, $K_{zp} = \frac{\kappa p_0 h_p}{z_a}$, $K_a = K_{gp}\mu$ and $K_b = \frac{\kappa R_s T_s}{z_b S}\mu$. We define the state variable $\boldsymbol{x} = [z, \dot{z}, p_a, p_b]^T$ and the state space equation is described as follows:

$$\dot{\boldsymbol{x}}(t) = \boldsymbol{A}_c \boldsymbol{x}(t) + \boldsymbol{B}_c u(t - L), \quad (15)$$

where $\boldsymbol{A}_c$ and $\boldsymbol{B}_c$ are defined as follows:

$$\boldsymbol{A}_c = \begin{bmatrix} 0 & 1 & 0 & 0 \\ -k_p/M & -c_p/M & S/M & 0 \\ 0 & -K_{zp} & -K_a & K_a \\ 0 & 0 & K_b & -K_b \end{bmatrix} \quad (16)$$

$$\boldsymbol{B}_c = \begin{bmatrix} 0 \\ 0 \\ K_{gp} \\ 0 \end{bmatrix}. \quad (17)$$

Input time delay $L = 20$ ms is described via the second order Pade approximation as follows:

$$e^{-Ls} = \frac{\frac{1}{12}L^2 s^2 - \frac{1}{2}Ls + 1}{\frac{1}{12}L^2 s^2 + \frac{1}{2}Ls + 1}. \quad (18)$$

The state space representation of (18) is described as follows:

$$\dot{\boldsymbol{x}}_{\boldsymbol{l}}(t) = \boldsymbol{A}_l \boldsymbol{x}_{\boldsymbol{l}}(t) + \boldsymbol{B}_l u(t), \quad \boldsymbol{x}_{\boldsymbol{l}}(t) = [x_{l1}(t), x_{l2}(t)]^T \quad (19)$$

$$y_l(t) = \boldsymbol{C}_l \boldsymbol{x}_{\boldsymbol{l}}(t) + D_l u(t), \quad y_l(t) := u(t - L) \quad (20)$$

$$\boldsymbol{A}_l = \begin{bmatrix} -3.0 \cdot 10^2 & -3 \cdot 10^4 \\ 1 & 0 \end{bmatrix}, \quad \boldsymbol{B}_l = \begin{bmatrix} 1 \\ 0 \end{bmatrix} \quad (21)$$

$$\boldsymbol{C}_l = \begin{bmatrix} -6 \cdot 10^2 & 0 \end{bmatrix}, \quad D_l = \begin{bmatrix} 1 \end{bmatrix}. \quad (22)$$

Subsequently, the plant including input time delay is described as follows:

$$\dot{\tilde{\boldsymbol{x}}}(t) = \tilde{\boldsymbol{A}}_{\boldsymbol{c}}\tilde{\boldsymbol{x}}(t) + \tilde{\boldsymbol{B}}_{\boldsymbol{c}}u(t) \quad (23)$$

$$\tilde{\boldsymbol{x}}(t) = [\boldsymbol{x}^T(t), x_{l1}, x_{l2}(t)]^T \quad (24)$$

$$\tilde{\boldsymbol{A}}_c = \begin{bmatrix} \boldsymbol{A}_c & \boldsymbol{B}_c \boldsymbol{C}_l \\ 0 & \boldsymbol{A}_l \end{bmatrix}, \quad \tilde{\boldsymbol{B}}_c = \begin{bmatrix} \boldsymbol{B}_c D_l \\ \boldsymbol{B}_l \end{bmatrix}. \quad (25)$$

$\tilde{\boldsymbol{A}}$ and $\tilde{\boldsymbol{B}}$ of the discretized plant in (1) are obtained via the discretization of (23) by assuming that the zero-order-hold is used with sampling T_u. In this case, the state space variable of (1) is as follows:

$$\tilde{\boldsymbol{x}}[k] = [\boldsymbol{x}^T[k], x_{l1}[k], x_{l2}[k]]^T, \quad (26)$$

where x_{l1} and x_{l2} denote the state variables of the input time delay. All of the state variables of $\tilde{\boldsymbol{x}}[k]$ are measurable. Moreover, the system is controllable. In many real systems, it is impossible to measure all the state variables. However, it is possible to obtain the signals of the state variables using devices such as pressure sensors or displacement sensors in the experimental setup.

The control input is quantized by the quantizer $\phi(\sigma)$. The quantized input is generated via a combination of the open or close states of the valves shown in Table 2. Subsequently,

Table 1. Plant parameter values

Displacement of the isolation table	z	[m]
Air spring pressure deviation	p_a	[Pa]
Buffer tank pressure deviation	p_b	[Pa]
Control input (mass flow rate)	u	[kg/s]
Primary pressure	p_0	0.0350[MPa]
Mass of the table	M	13.6[kg]
Equiv. spring constant	k_p	14.5×10^3[N/m]
Equiv. damping coefficient	c_p	43.6[Ns/m]
Contact area of air spring	S	3.60×10^{-3}[m^2]
Gas constant	R_s	287[J/(kg·K)]
Ratio of specific heat	κ	1.4[-]
Gas temperature	T_s	293[K]
Valve coefficient	μ	2.90×10^{-7}[kg/(s· Pa)]
Time-delay of mass flow rate	L	20[ms]
Equiv. air spring height	z_a	0.0120[m]
Equiv. buffer tank height	z_b	0.308[m]
Volume conversion coefficient	h_p	2[-]
Max. mass flow rate	G_{1+}	2.70×10^{-4}[kg/s]
Min. mass flow rate	G_{1-}	-2.57×10^{-4}[kg/s]

Table 2. Driving pattern of the solenoid valve

	Val. #1	Val. #2	Val. #3	Val. #4	Control input
Inflow	On	-	-	-	G_{1+}
Outflow	-	-	On	On	G_{1-}
	-	-	-	-	0

On: Valve is open. -:Valve is closed.

the quantizer ϕ provides the following admissible three valued input.

$$\phi(\sigma) = \begin{cases} G_{1+} & , \text{ if } \quad \sigma_{1+} \le \sigma \\ G_{1-} & , \text{ if } \quad \sigma \le \sigma_{1-} \\ 0 & , \text{ others} \end{cases}, \quad (27)$$

where $\sigma[k]$ denotes the input of ϕ, and σ_{1+} and σ_{1-} denote the design parameters. We specify the parameters as $\sigma_{1+} = G_{1+}/2$ and $\sigma_{1-} = G_{1-}/2$.

6. CONTROL DESIGN AND NUMERICAL SIMULATIONS

6.1 Control design via the conventional method

The control was designed by assuming that $T_u = T_y$ and is based on the method proposed by Koike et al., (2013). The discretized plant was obtained by assuming that the sampling period is $T_u = T_y = 20$ ms in (23). Based on the method in Koike et al., (2013), the state feedback gain $\boldsymbol{F}_1$ was obtained by solving LQ optimal control problem by assuming the following weighting matrices.

$$\begin{cases} \boldsymbol{Q} = \text{diag}(1 \cdot 10^9, 5 \cdot 10^6, 4 \cdot 10^{-5} \\ \qquad\qquad , 4 \cdot 10^{-5}, 1 \cdot 10^7, 1 \cdot 10^7) \\ \boldsymbol{R} = 1 \end{cases} \quad (28)$$

By using MATLAB®, $\boldsymbol{F}_1$ was obtained as follows: $\boldsymbol{F}_1 = [-9.08 \cdot 10^{-1}, 2.35 \cdot 10^{-2}, 2.49 \cdot 10^{-8}, 4.35 \cdot 10^{-7}, 1.30 \cdot 10^0, 4.19 \cdot 10^4]$. Subsequently, $\tilde{\boldsymbol{A}} - \tilde{\boldsymbol{B}}\boldsymbol{F}_1$ corresponds to Hurwitz. The positive matrix $\boldsymbol{P}_1$ was obtained by solving the Lyapunov equation of (5) assuming $\boldsymbol{Q}_L = \boldsymbol{I}_6$. The control input is selected based on the value of (4), and control law Φ_1 is described as follows:

$$\Phi_1 : u[k] = \begin{cases} u[k] & , \text{ if } \Delta V < 0 \\ 0 & , \text{ otherwise} \end{cases}, \quad (29)$$

where $u[k]$ is specified by $\sigma[k] = -\boldsymbol{F}_1\tilde{\boldsymbol{x}}[k]$ and (2). Additionally, ΔV is as follows:

$$
\begin{aligned}
\Delta V[k] &= V[k+1] - V[k] \\
&= \tilde{\boldsymbol{x}}^T[k+1]\boldsymbol{P}_1\tilde{\boldsymbol{x}}[k+1] - \tilde{\boldsymbol{x}}^T[k]\boldsymbol{P}_1\tilde{\boldsymbol{x}}[k] \\
&= (\tilde{\boldsymbol{A}}\tilde{\boldsymbol{x}}[k] + \tilde{\boldsymbol{B}}u[k])^T\boldsymbol{P}_1(\tilde{\boldsymbol{A}}\tilde{\boldsymbol{x}}[k] + \tilde{\boldsymbol{B}}u[k]) \\
&\quad - \tilde{\boldsymbol{x}}^T[k]\boldsymbol{P}_1\tilde{\boldsymbol{x}}[k].
\end{aligned}
\tag{30}
$$

6.2 Control design via the proposed method

The proposed control described in Section 4 is applied to the pneumatic isolation control system. It was assumed that the sampling period for the measurement was $T_y = 20$ ms and that for the control was $T_u = 5$ ms. Therefore, $n = T_y/T_u = 4$. The $n = 4$ is specified such that the value is less than the order of the state variable of the plant $N = 6$ to ensure the convexity of J in (10). The plant and state variable are (1) and (26), respectively. The plant was discretized via the sampling period $T_u = 5$ ms in (23). The feedback gain in Section 4.2, $\boldsymbol{F}$, was designed by solving the LQ optimal control problem using MATLAB®, and we specified the weightings to be the same as Q and R in (28). The obtained feedback gain was $\boldsymbol{F} = \boldsymbol{F}_2 = [-2.04 \cdot 10^0, 1.17\cdot10^{-1}, 8.42\cdot10^{-8}, 1.22\cdot10^{-6}, 7.16\cdot10^1, 1.46\cdot10^5]$. By $\boldsymbol{F}_2$, $\tilde{\boldsymbol{A}} - \tilde{\boldsymbol{B}}\boldsymbol{F}_2$ corresponds to Hurwitz, and the positive matrix $\boldsymbol{P}_2$ was obtained by solving the Lyapunov equation with $\boldsymbol{Q}_L = \boldsymbol{I}_6$.

6.3 Numerical simulations by the conventional method

Numerical simulations were performed for the conventional method for the pneumatic isolation control system model. The designed control for the conventional method is shown in the previous section. Impulse disturbance responses were obtained. Examples of control responses by the conventional method described in Section 6.1 are shown in Fig. 8 and Fig. 9. The sampling period for Fig. 8 is $T_u = T_y = 5$ ms while the one for Fig. 9 is $T_u = T_y = 20$ ms. The discretized plant for each simulation was obtained by assuming each sampling period T_u in (23). Feedback gains for Fig. 8 and Fig. 9 are specified as $\boldsymbol{F}_2$ and $\boldsymbol{F}_1$, respectively. The responses correspond to the simulation results by the linearized model shown in Section 5. In the figures, the solid lines denote the responses of the plant with discretized control input. The dashed lines denote the responses of the plant although $u[k] = \phi(\sigma[k]) = \sigma[k]$ and $u[k] = -\boldsymbol{F}_i\tilde{\boldsymbol{x}}[k], (i = 1, 2)$ corresponds to a continuous control input. In Fig. 8, the discretized control input response is slightly more deteriorated compared with the continuous control input although both the responses provide good convergence properties. Conversely, the discretized control provides the significantly deteriorated response shown in Fig. 9 compared with the continuous control input. The deteriorated response is attributed to the excessive coarseness of the smallest resolving power of the control input (which was restricted by the sampling period of 20 ms and the coarse quantizer shown in Fig. 1).

6.4 Numerical simulations by the proposed method

Impulse disturbance responses were obtained for the proposed method as well as the conventional method. The
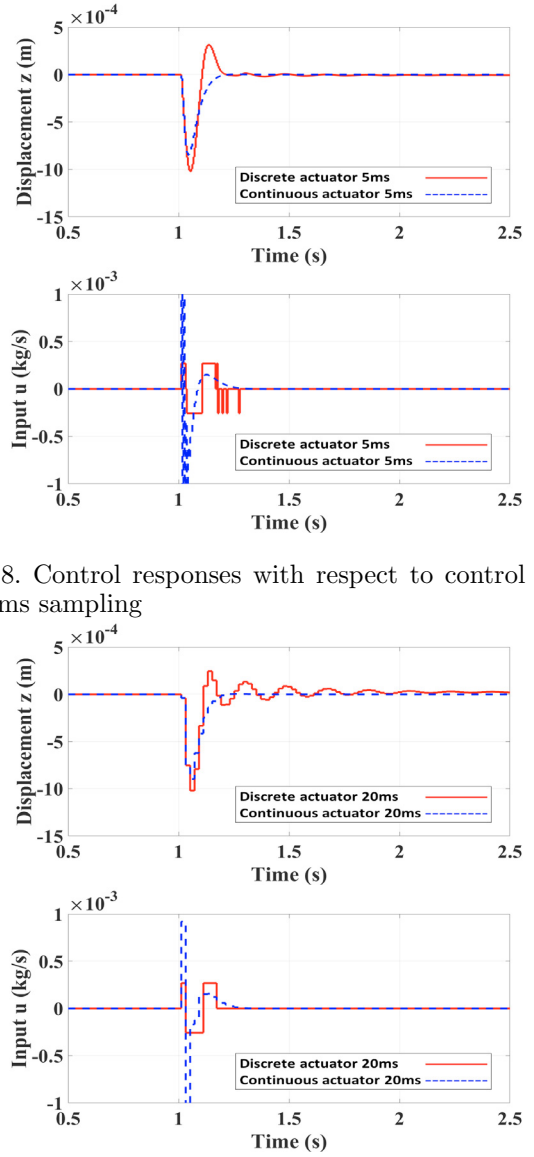

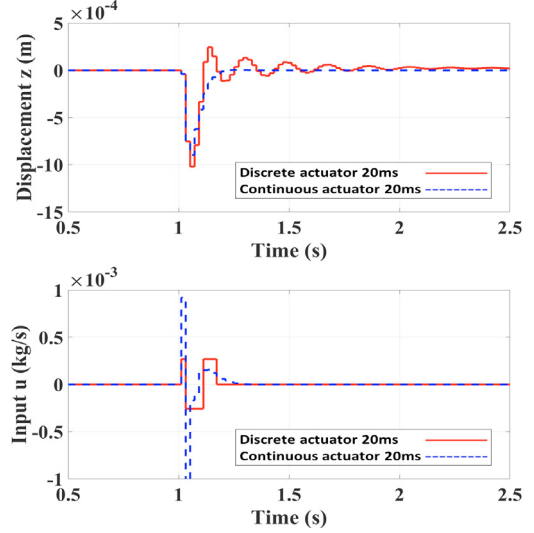Fig. 8. Control responses with respect to control with 5 ms sampling

Fig. 9. Control responses with respect to control with 20 ms sampling

obtained simulation results are shown in Fig. 10. The upper figure denotes the response of the displacement z, and the lower figure denotes the control inputs. In each figure, the solid line denotes the response of the proposed method and the dashed line denotes that of the conventional method. The performance of the proposed method is superior to that of the conventional method. The essense of the proposed method is that it makes the resolution of the control input value finer.

If the sampling period is specified such that $T_y = T_u = 5$ ms in the conventional method, then we obtain the responses in the solid line in Fig. 8. The response is similar to that of the proposed method shown in Fig. 10. This implies that we can consider a relatively low sampling frequency for the output measurement although it is necessary to specify a relatively high sampling frequency for the control input in the case of the plant with the quantized input such as the plant in the present study. Therefore, the proposed method is effective in cases wherein we do not consider a high sampling frequency for the output measurement
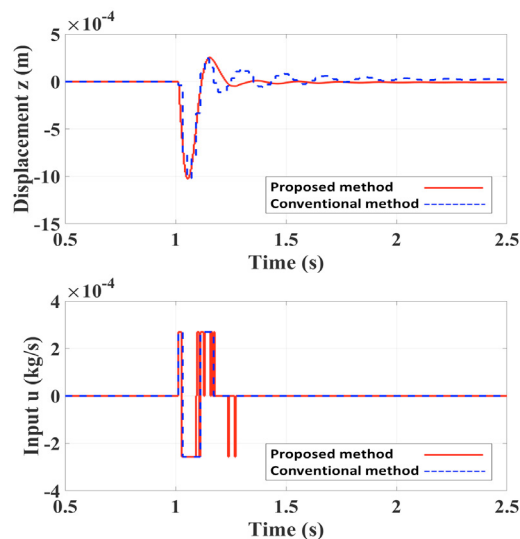
Fig. 10. Simulation results for impulse disturbance response

although it is possible to consider a short sampling interval for control input.

We verified that the control law of the proposed method can be easily implemented with respect to the real-time controller in the experimental system. The maximum calculation time to obtain a control input was 7.24 ms with the proposed method. The calculation cost is sufficiently small and easily implemented in real controllers. The simulation was conducted by a CPU equipped with Intel®Core i7 with 4 GHz and 8 GB RAM.

7. CONCLUSION

The results of the study indicated that control performance deteriorated for a discrete input valued plant in a few cases if a relatively low sampling frequency is used. The findings suggested that multirate control by using high input frequency is effective in terms of improving the control performance in case of the low sampling frequency for measurement. Furthermore, the MPC based method to determine the high sampling input was applied. The effectiveness of the proposed method was verified via numerical simulations. The authors thank the reviewers for their kind suggestions.

REFERENCES

Azuma, S., and Sugie, T. (2007). Synthesis of Optimal Dynamic Quantizers for Symbolic Input Control. *Transactions of the Institute of Systems, Control and Information Engineers*, 20, 122–129(in Japanese).

Azuma, S., and Sugie, T. (2008). Synthesis of Optimal Dynamic Quantizers for Discrete-Valued Input Control. *IEEE Transactions on Automatic Control*, 53, 2064–2075.

Fujimoto, H. (2009). Application of multirate sampling control to robot manipulator. *Jounal of the Robotics Society of Japan*, 27, 410–413(in Japanese).

Ishikawa, M., Murata, I., and Sugie, T. (2007). Quantized Controller Design Using Feedback Modulators. *Transactions of the Society of Instrument and Control Engineers*, 43, 31–36(in Japanese).

James, B.R., and Michael, J.R. (2017). Model predictive control with discrete actuators: Theory and application. *Automatica*, 78, 258–265.

Jong, O.S., and Kwang, J.K. (2013). Control of transient vibrations due to stage movements in 6-dof active pneumatic table by inertial force compensation. *Journal of Sound and Vibration*, 332, 5241–5254.

Kato, T., Kawashima, K., Sawamoto, K., and Kagawa, T. (2007). Active control of a pneumatic isolation table using model following control and a pressure differentiator. *Precision Engineering*, 31, 269–275.

Kato, T., Kawashima, K., Funaki, T., Tadano, K., and Kagawa, T. (2010). A new, high precision, quick response pressure regulator for active control of pneumatic vibration isolation tables. *Precision Engineering*, 34, 43–48.

Kawashima, K., Kato, T., Sawamoto, K., and Kagawa, T. (2007). Realization of virtual sub chamber on active controlled pneumatic isolation table with pressure differentiator. *Precision Engineering*, 31, 139–145.

Kobayashi, K., Wai, W.S., and Hiraishi, K. (2014). Large scale MPC with continuous/discrete-valued inputs: Compensation of quantization errors, stabilization, and its application. *SICE Journal of Control, Measurement, and System Integration*, 7(3), 31–36.

Koike, M., and Chida, Y. (2012). Multivariate Control Design Considering Quantization Error and Input Time-Delay for Pneumatic Isolation Table. *The American Society of Mechanical Engineers*, 3, 783–792. ASME 2012 5th Annual Dynamic Systems and Control Conference joint with the JSME 2012 11th Motion and Vibration Conference.

Koike, M., Chida, Y., and Ikeda, Y. (2013). Control of a Pneumatic Isolation Table Including Non-linear Quantizer. *Transactions of the Society of Instrument and Control Engineers*, 49(4), 488–496(in Japanese).

Marcel, H., and Nathan, V.D.W. (2006). Nonlinear Dynamics and Control of a Pneumatic Vibration Isolator. *Journal of Vibration and Acoustics*, 128, 439–448.

Martin, C.B., N, Amit., and J, D.Powell. (1988). Multirate digital control system design. *IEEE Transaction on Automatic Control*, 33(12), 1139–1150.

Maruyama, N., Chida, Y., and Ikeda, Y. (2013). Model Predictive Control of Pneumatic Isolation Table with Quantized Input. *SICE Annual Conference 2013*, 727–732. 2013 the SICE Annual Conference 2013.

Maruyama, N., Koike, M., and Chida, Y. (2015). Model Predictive Control Method for Pneumatic Isolation Table with Discrete-Valued Input. *Transactions of the Society of Instrument and Control Engineers*, 51, 755–762(in Japanese).

Minami, Y., Azuma, S., and Sugie, T. (2007). Optimal Dynamic Quantizers in Discrete-Valued Input Feedback Control Systems. *Transactions of the Society of Instrument and Control Engineers*, 43(3), 227–233(in Japanese).

Sawada, K., and Shin, S. (2010). Dynamic Quantizer Synthesis Based on Invariant Set Analysis for SISO Systems with Discrete-Valued Input. *Transactions of the Institute of Systems, Control and Information Engineers*, 23(11), 249–256(in Japanese).